

Supporting Information

Improving the Carrier Stability and Drug Loading of Unimolecular Micelle-based Nanotherapeutic for Acid- activated Drug Delivery and Enhanced Antitumor Therapy

*Xiaoxiao Shi^{a, b}, Shuang Bai^{a, b}, Cangjie Yang^c, Xiaoqian Ma^{a, b}, Meili Hou^{a, b}, Jiucun
Chen^{a, b}, Peng Xue^{a, b}, Chang Ming Li^{a, b}, Yuejun Kang^{a, b*}, Zhigang Xu^{a, b*}*

^aInstitute for Clean Energy and Advanced Materials, Faculty of Materials and Energy,
Southwest University, Chongqing 400715, P. R. China

^bChongqing Engineering Research Centre for Micro-Nano Biomedical Materials and
Devices, Chongqing 400715, P.R. China.

^cSchool of Chemical and Biomedical Engineering, Nanyang Technological
University, 62 Nanyang Drive, Singapore 637459, Singapore

*Corresponding Authors

Z. Xu (zgxu@swu.edu.cn); Fax: +86-23-68253204; Tel: +86-23-68253792

Y. Kang (yjkang@swu.edu.cn); Fax: +86-23-68253204; Tel: +86-23-68254056

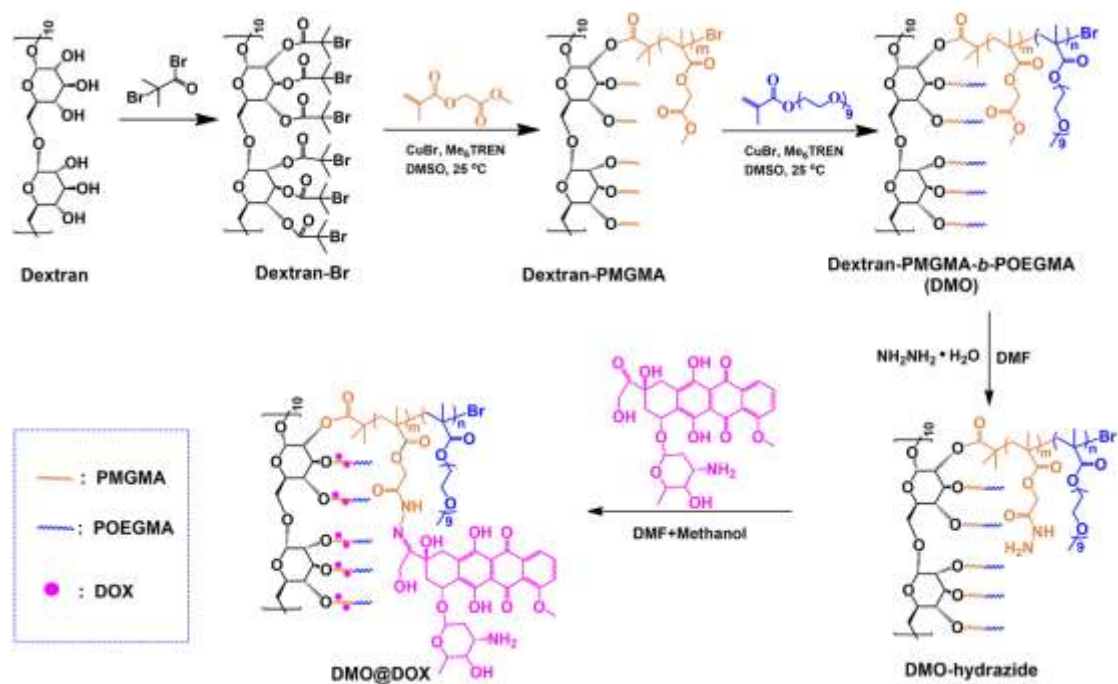


Figure S1. The synthetic route of rod-like DMO@DOX polymeric prodrug.

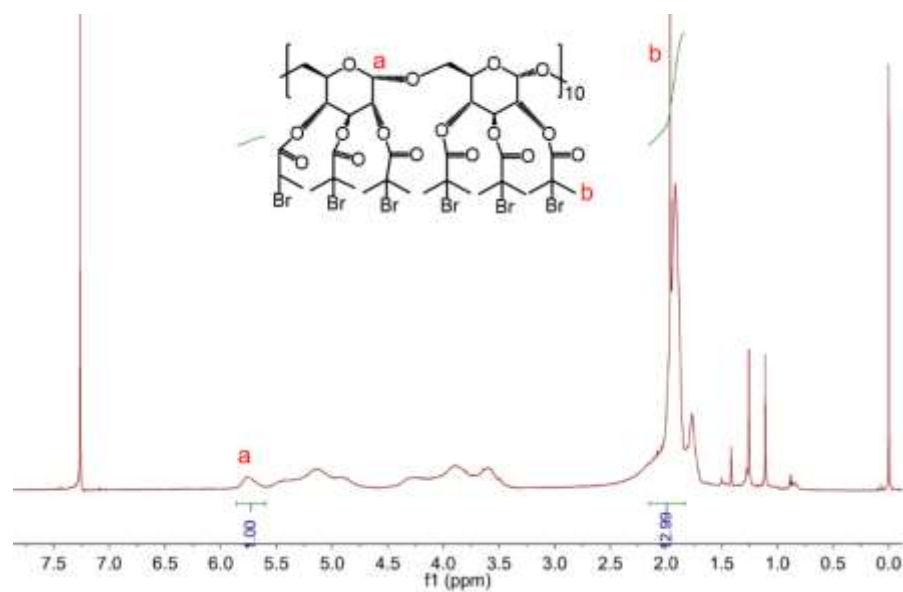


Figure S2. The ^1H NMR spectrum of DEX-Br macroinitiator.

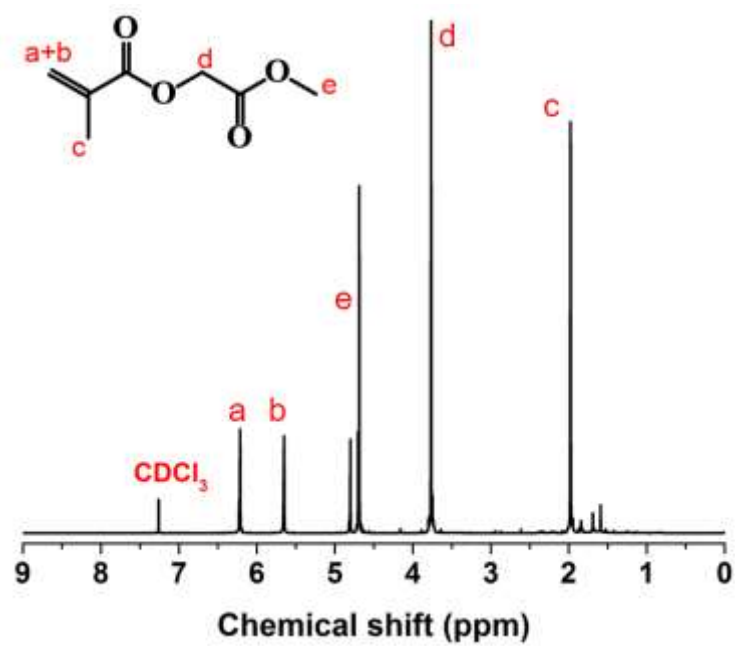


Figure S3. The ^1H NMR spectrum of MGMA monomer.

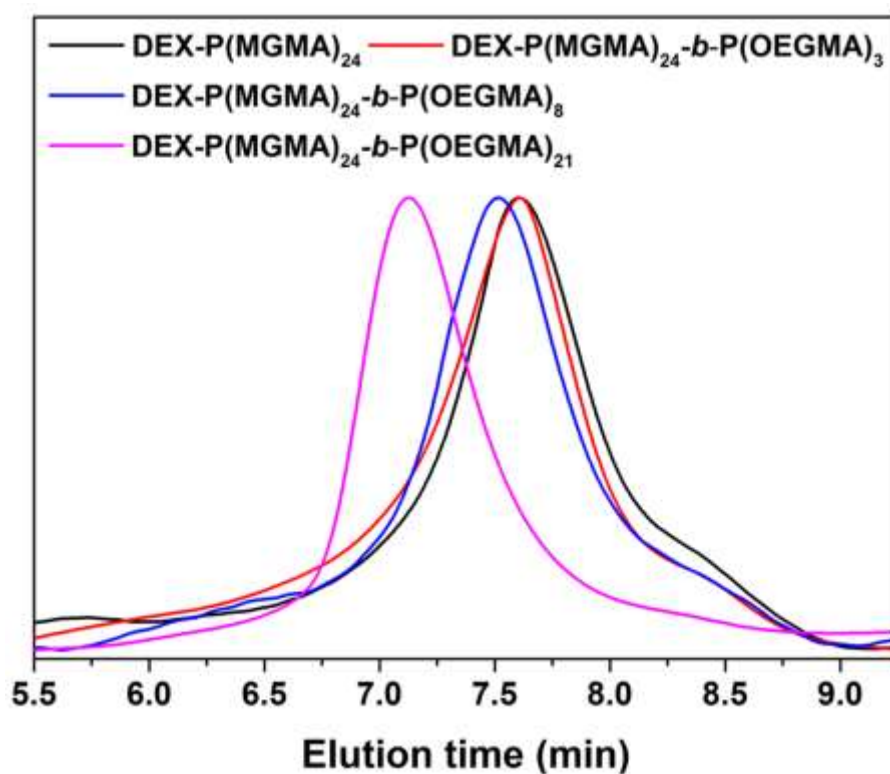


Figure S4. GPC traces of DEX-PMGMA₂₄ and DEX-P(MGMA)₂₄-*b*-P(OEGMA)₃ (DMO-1), DEX-P(MGMA)₂₄-*b*-P(OEGMA)₈ (DMO-2) and DEX-P(MGMA)₂₄-*b*-P(OEGMA)₂₁ (DMO-3).

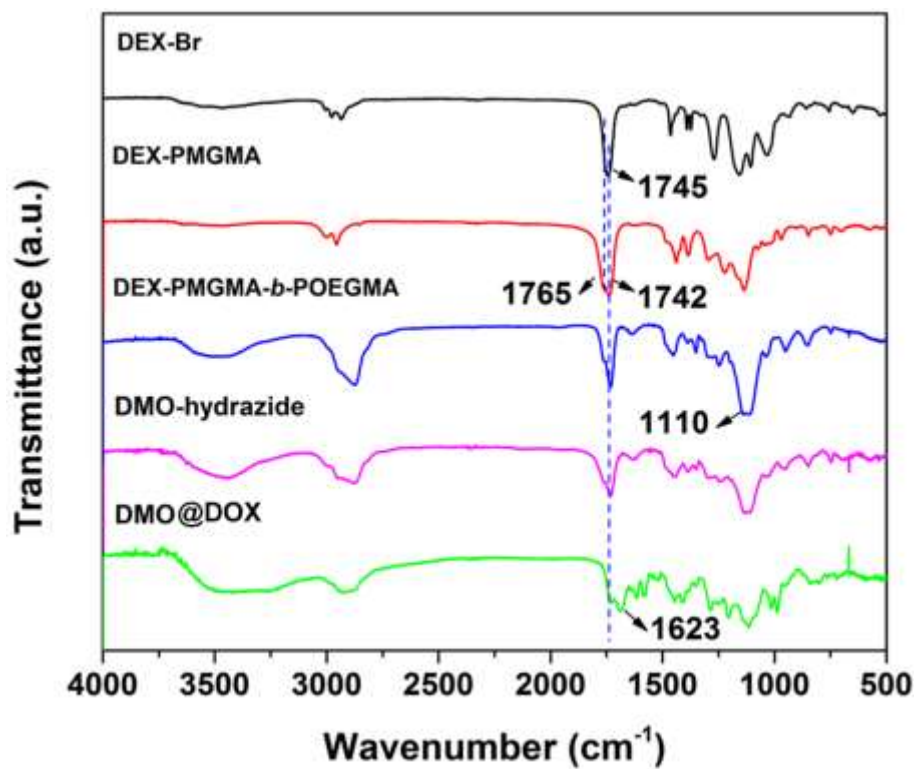


Figure S5. Typical FTIR spectra of DEX-Br, DEX-PMGMA, DEX-PMGMA-*b*-POEGMA (DMO), DMO-hydrazide and DMO@DOX, respectively.

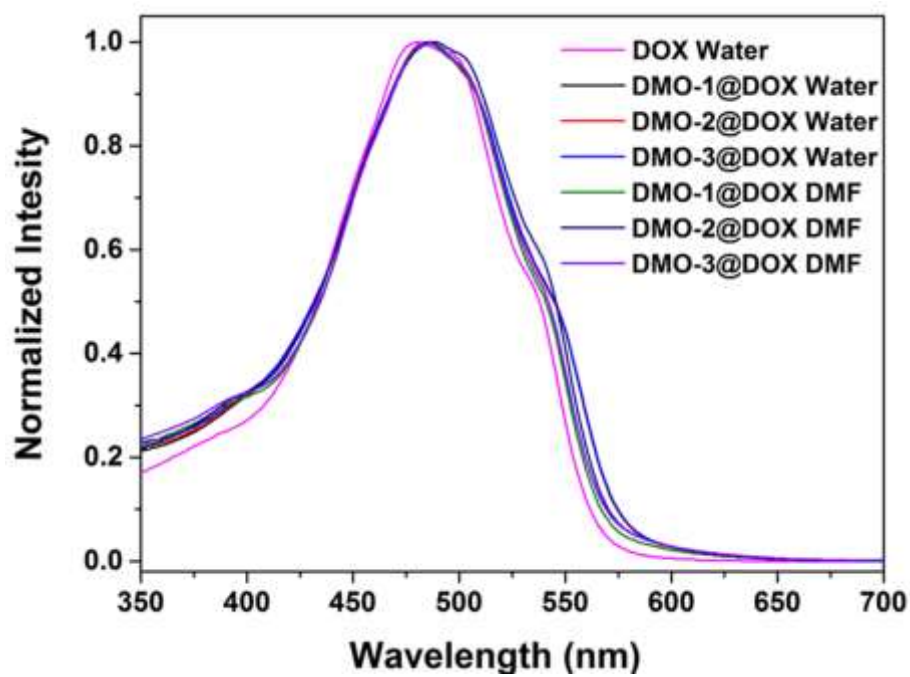


Figure S6. UV-vis spectra of free DOX, DMO-1@DOX, DMO-2@DOX and DMO-3@DOX prodrugs in water or DMF solution.

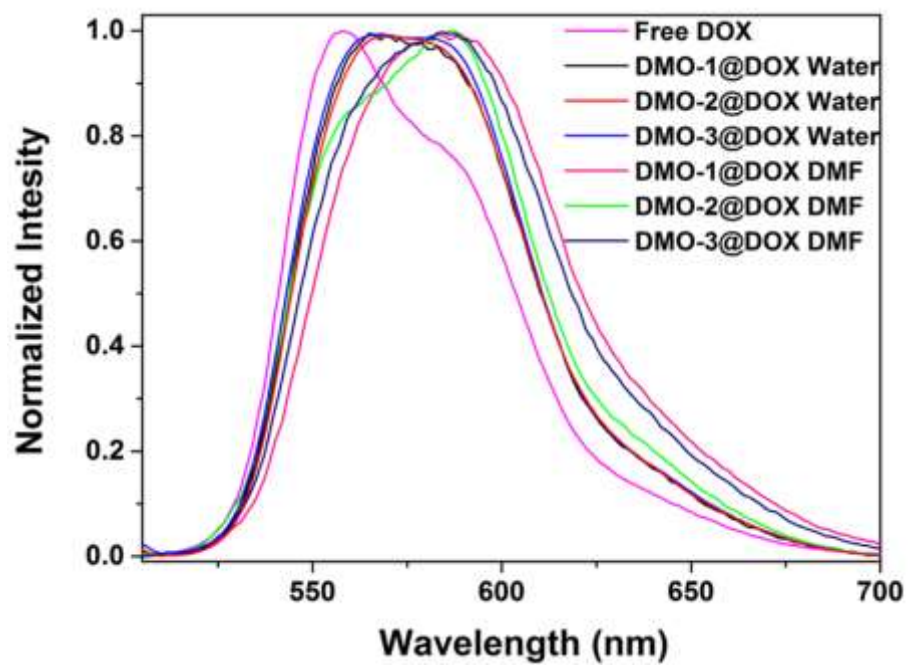


Figure S7. The fluorescence spectra of free DOX, DMO-1 @DOX, DMO-2@DOX and DMO-3@DOX prodrugs in water or DMF solution.

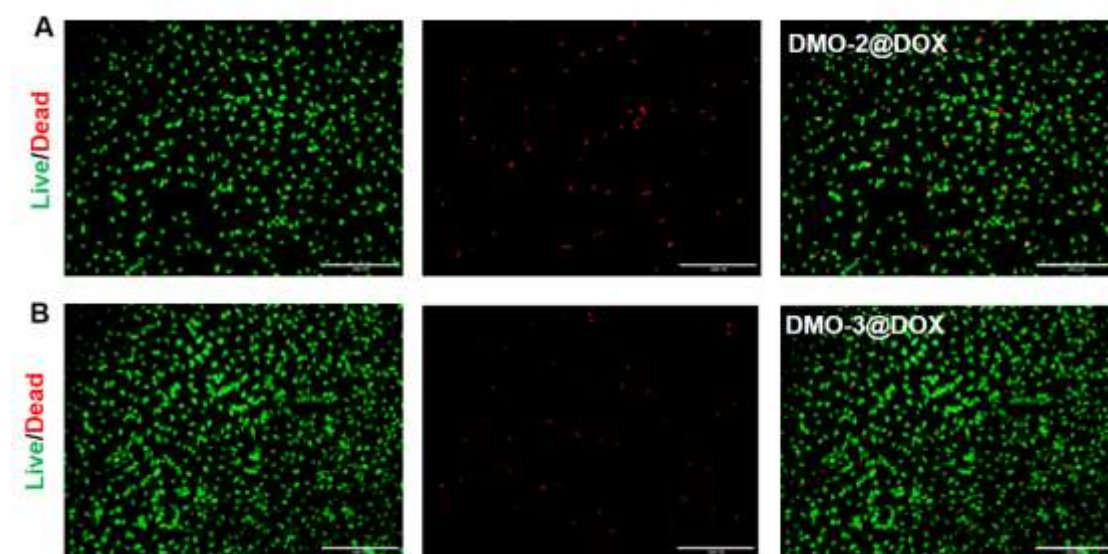


Figure S8. Fluorescence images of HeLa cells incubated with (A) DMO-2@DOX UMIs and (B) DMO-3@DOX UMIs for 24 h, respectively (final equivalent DOX concentration: 15 $\mu\text{g/mL}$). The fluorescence of Calcein AM (live cells) and PI (dead cells) were labelled as green and red, respectively. Scale bars: 200 μm .

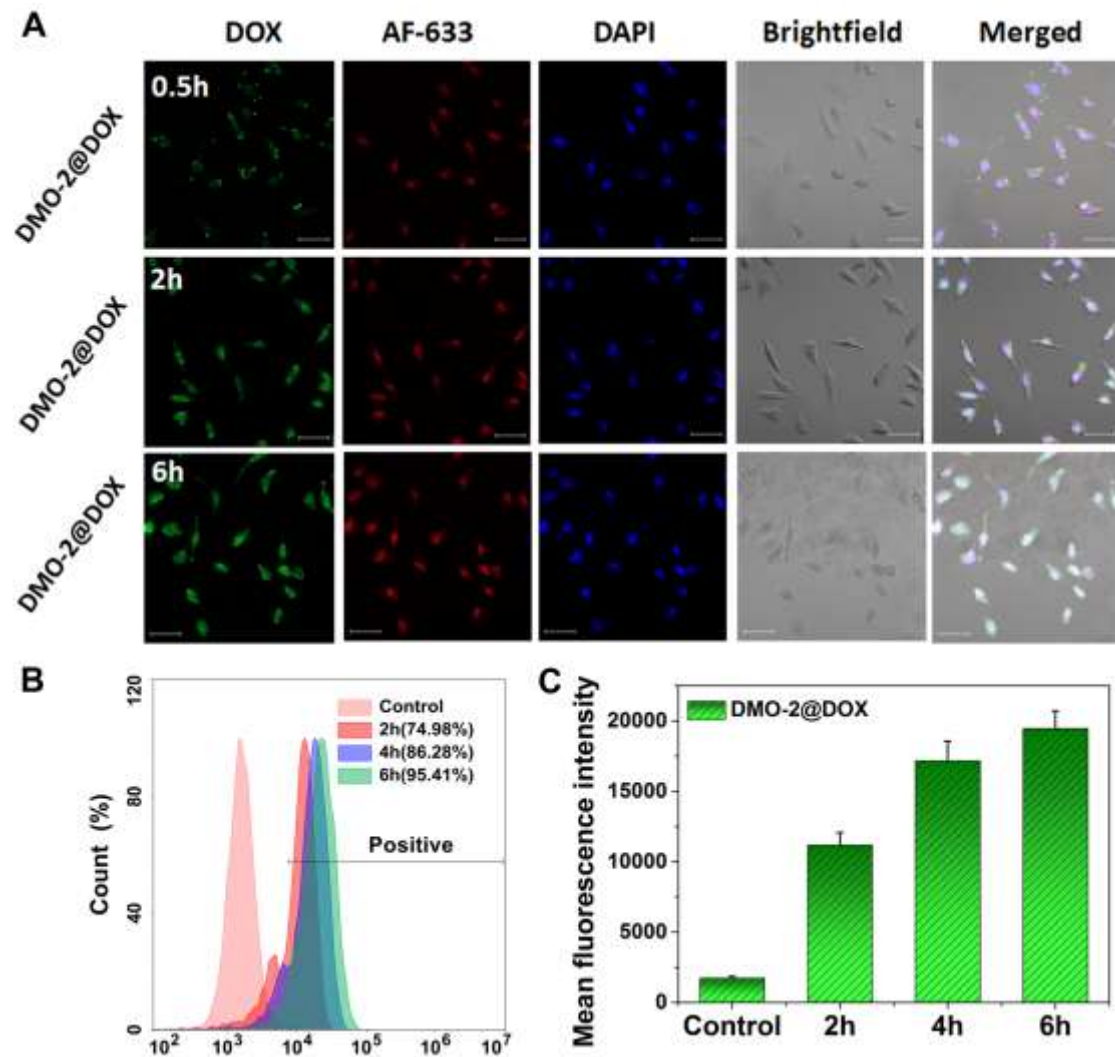


Figure S9. (A) CLSM images showing the distribution of free DOX and DMO-2@DOX UMs in HeLa cells (final equivalent DOX concentration: 20 $\mu\text{g/mL}$). Cell nuclei and cytoplasm were stained with DAPI (Blue) and AF-633 (Red), respectively. Scale bars: 50 μm . (B) Flow cytometry analysis and (C) the mean fluorescence intensity of DMO-2@DOX treated HeLa cells at 2, 4 and 6 h (data are presented as means \pm SD, $n=3$).

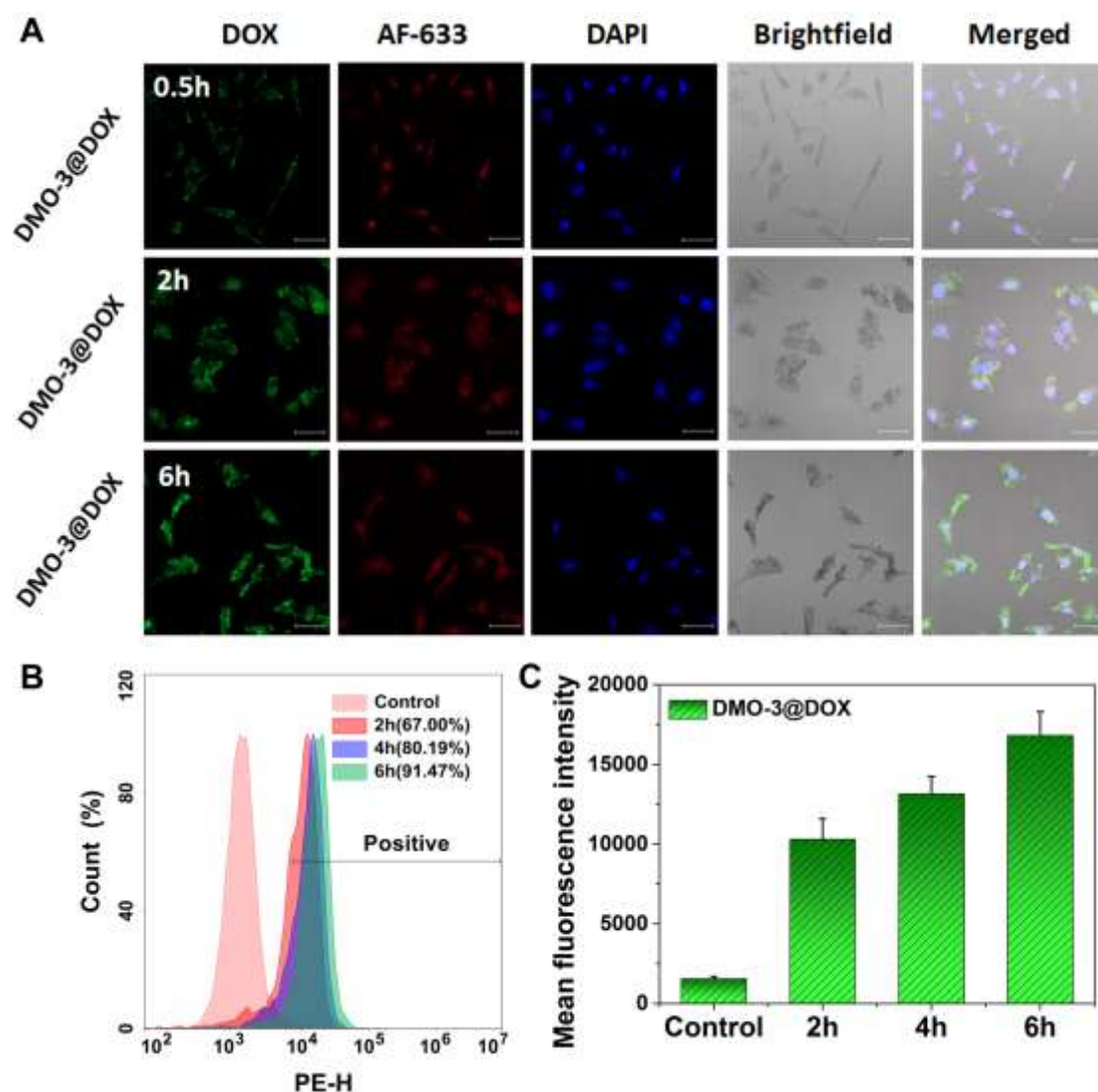


Figure S10 (A) CLSM images showing the distribution of free DOX and DMO-3@DOX UMs in HeLa cells (final equivalent DOX concentration: 20 $\mu\text{g/mL}$). Cell nuclei and cytoplasm were stained with DAPI (Blue) and AF-633 (Red), respectively. Scale bars: 50 μm . (B) Flow cytometry analysis and (C) the mean fluorescence intensity of DMO-3@DOX treated HeLa cells at 2, 4 and 6 h (data are presented as means \pm SD, $n=3$).

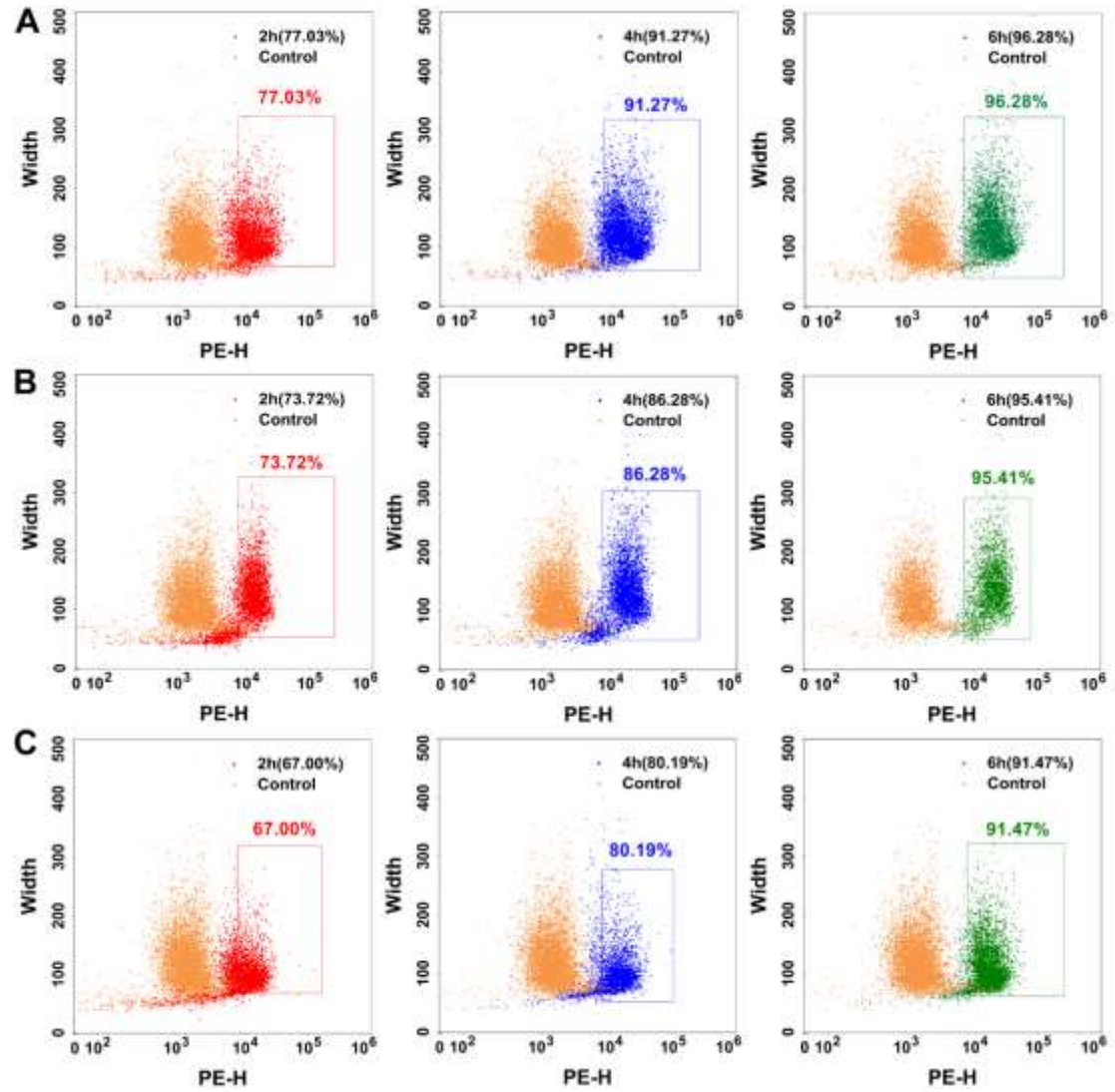


Figure S11 Flow cytometry dot plots for HeLa cells treated with (A) DMO-@DOX, (B) DMO-2@DOX and (C) DMO-3@DOX UMIs under different incubation time.

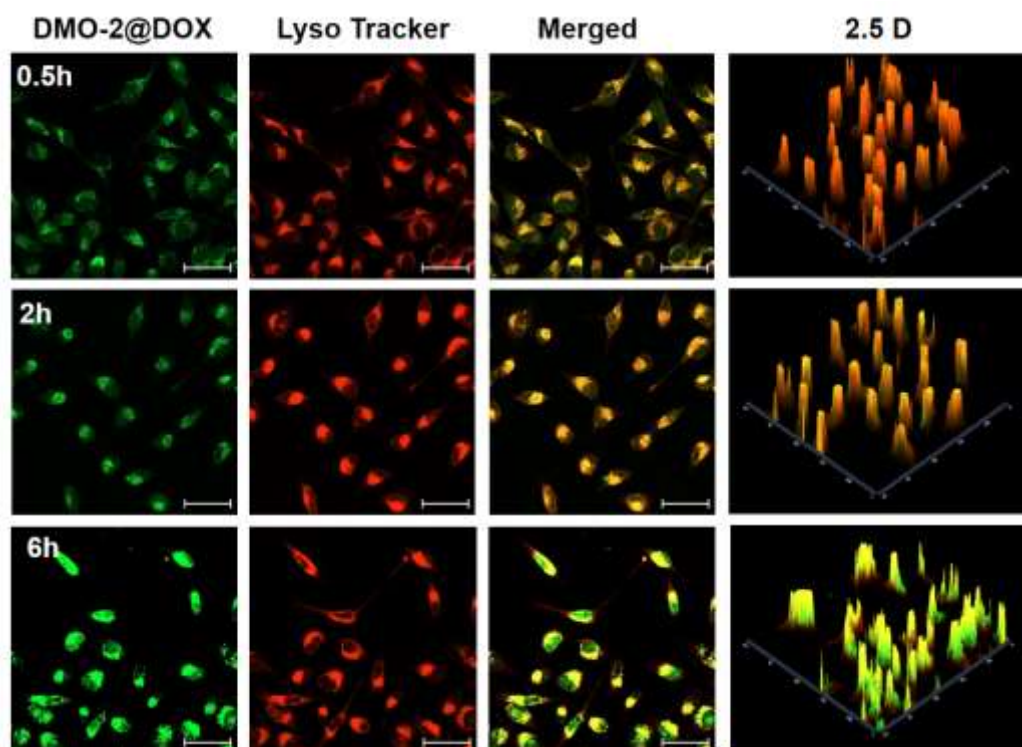


Figure S12 CLSM images showing the time-dependent accumulation process of DMO-2@DOX UMs using Lyso Tracker as the tracer (final equivalent DOX concentration: 20 $\mu\text{g/mL}$). Scale bars: 50 μm .

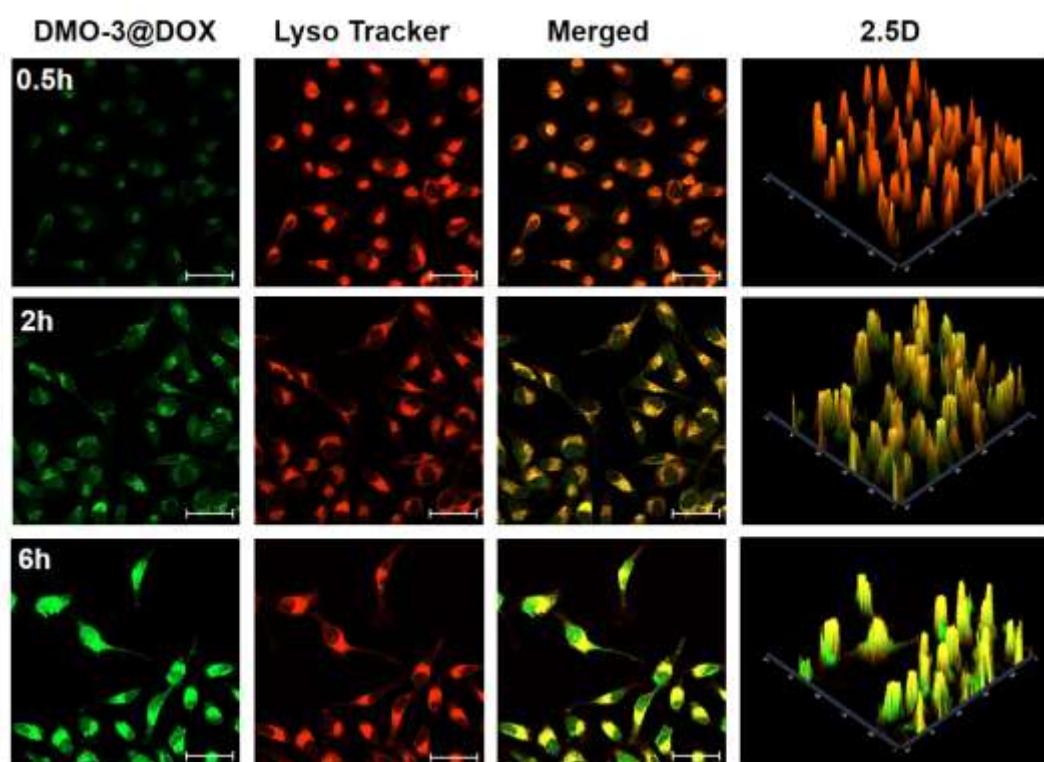


Figure S13 CLSM images showing the time-dependent accumulation process of DMO-2@DOX UMs using Lyso Tracker as the tracer (final equivalent DOX concentration: 20 $\mu\text{g/mL}$). Scale bars: 50 μm .

Table S1. Structural information of the rod-like DMO@DOX prodrug and their precursors

	$M_{n, NMR}^b$	$M_{n, GPC}^c$	M_w/M_n^d	D^e	D^f	LC^g (wt%)
Polymer ^a	(g mol ⁻¹)	(g mol ⁻¹)		(Water)	(DMF)	
DEX-P(MGMA) ₂₄	252900	38900	1.46	—	—	—
DEX-P(MGMA) ₂₄ - <i>b</i> -P(OEGMA) ₃	339200	42900	1.56	34.83	45.89	80.4
DEX-P(MGMA) ₂₄ - <i>b</i> -P(OEGMA) ₈	496900	48500	1.28	41.35	55.96	72.2
DEX-P(MGMA) ₂₄ - <i>b</i> -P(OEGMA) ₂₁	912200	95500	1.24	68.01	74.23	40.4

^a DP_n of polymerized alternating units (MGMA or OEGMA) and ^b $M_{n, NMR}$ was measured by ¹H NMR results. ^c $M_{n, GPC}$ and ^d M_w/M_n were measured by GPC. ^e Hydrodynamic diameter of prodrug micelles were determined by DLS. ^f The loading content (LC) were determined by Fluorescence (FL) spectrophotometer, respectively.

Table S2. IC₅₀ value of free DOX and DMO@DOX prodrug. ^a

Sample	IC ₅₀ (HeLa)	IC ₅₀ (MCF-7)	IC ₅₀ (HUVEC)
	μg/ml	μg/ml	μg/ml
Free DOX	0.072	0.06	0.075
DMO-1@DOX	1.61	0.77	>10
DMO-2@DOX	0.65	1.75	>10
DMO-3@DOX	0.83	1.91	>10

a: IC₅₀ value of free DOX, DMO-1@DOX, DMO-2@DOX and DMO-3@DOX determined in HeLa cells, MCF-7 cells and HUVEC cells by PrestoBlue assay, and cells were incubated with samples for 72 h.